Mineralogical Magazine, December 2010, Vol. 74(6), pp. 969–978

Jahnsite–whiteite solid solutions and associated minerals in the phosphate pegmatite at Hagendorf-Süd, Bavaria, Germany

I. E. Grey[1,*], W. G. Mumme[1], S. M. Neville[1], N. C. Wilson[1] and W. D. Birch[2]

[1] CSIRO Process Science and Engineering, Box 312 Clayton South, Victoria 3169, Australia
[2] Geosciences, Museum Victoria, GPO Box 666, Melbourne 3001, Victoria, Australia

[*Received 5 November 2010; Accepted 24 November 2010*]

ABSTRACT

Secondary phosphate assemblages from the Hagendorf Süd granitic pegmatite, containing the new Mn-Al phosphate mineral, nordgauite, have been characterized using scanning electron microscopy and electron microprobe analysis. Nordgauite nodules enclose crystals of the jahnsite–whiteite group of minerals, showing pronounced compositional zoning, spanning the full range of Fe/Al ratios between jahnsite and whiteite. The whiteite-rich members are F-bearing, whereas the jahnsite-rich members contain no F. Associated minerals include sphalerite, apatite, parascholzite, zwieselite-triplite solid solutions and a kingsmountite-related mineral. The average compositions of whiteite and jahnsite from different zoned regions correspond to jahnsite-(CaMnMn), whiteite-(CaMnMn) and the previously undescribed whiteite-(CaMnFe) end-members. Mo-$K\alpha$ CCD intensity data were collected on a twinned crystal of the (CaMnMn)-dominant whiteite and refined in $P2/a$ to wR_{obs} = 0.064 for 1015 observed reflections.

Keywords: jahnsite–whiteite solid solutions, Hagendorf pegmatite, kingsmountite analogue, nordgauite, secondary phosphate minerals.

Introduction

The Hagendorf Süd granitic pegmatite (49º39′1″N, 12º27′35″E) is a renowned source of phosphate minerals, particularly secondary phosphates. A recent compilation of minerals identified at Hagendorf reports 174 valid species, of which 11 are type specimens. Of these, nine are secondary phosphates: jungite, keckite, laueite, lehnerite, parascholzite, pseudolaueite, scholzite, strunzite and wilhelmvierlingite (Kastning and Schlüter, 1994). We have recently identified another new secondary phosphate mineral, with composition $MnAl_2(PO_4)_2(F,OH)_2.5.5H_2O$, in Hagendorf Süd hand specimens from the Cornelia Mine Open Cut (at 67 metres), supplied by Erich Keck. The mineral and its name, nordgauite, have been approved by the IMA CNMNC, 2010-040 (Birch *et al.*, 2010).

Nordgauite occurs in two different forms, as mm-sized rounded waxy nodules (compact form) or as sub-spherical fibrous aggregates (fibrous form). Both forms occur in small cavities etched in zwieselite-triplite, $M_2PO_4(OH)$, where M = Fe or Mn. In a scanning electron microscope (SEM) examination of nordgauite occurrences we observed numerous small inclusions of lath-like crystals, which electron microprobe (EMP) analyses showed were consistent with members of the jahnsite–whiteite family of minerals (Moore and Ito, 1978). These have the general formula $XM(1)M(2)_2M(3)_2(PO_4)_4(OH)_2.8H_2O$, with $M(3)$ = Fe^{3+} and Al^{3+}, respectively, for jahnsite and whiteite end-members, X = Ca, Na, Mn and $M(1)$, $M(2)$ are commonly divalent Mn, Fe, Mg and Zn. An unusual aspect of the lath-like crystals is the presence of compositional zoning, spanning the full range from jahnsite to whiteite. Moore and Ito (1978) had noted that "there was

* E-mail: ian.grey@csiro.au
DOI: 10.1180/minmag.2010.074.6.969

no evidence as yet that solid solutions between the two is extensive" and subsequent publications on new species of jahnsite and whiteite have generally not shown significant compositional Fe/Al mixing in *M*(3).

Whiteite laths were also found growing from the walls of the small cavities containing the fibrous nordgauite aggregates. One of these, though twinned, was used for single-crystal X-ray data collection. We report here the characterization of the jahnsite–whiteite solid solutions and associated minerals from EMP analyses and a crystal structure refinement on CaMnMn-dominant whiteite from the Hagendorf Süd deposit.

Experimental

Samples taken from hand specimens from the Cornelia Mine Open Cut at 67 metres, supplied by Dr Erich Keck, were mounted in epoxy blocks, polished and carbon-coated for examination by SEM and for EMP analysis. The analyses were conducted in wavelength-dispersive mode using a JEOL 8500 Hyperprobe operated at an accelerating voltage of 15 kV, a beam current of 10 nA and a beam defocus of 2 μm. The reference materials used were fluorite, CaF_2, for Ca and F; $AlPO_4$ for P; $MgAl_2O_4$ for Mg and Al; ZnS for Zn; hematite for Fe; and Mn metal and albite for Na. The EMP results are listed in Table 1. All jahnsite-whiteite contains 8 molecules of water which constitutes ~20 wt.%.

Whiteite crystals from the cavity walls were examined using oscillation/Weissenberg and precession photographs. The crystals were generally of poor quality, exhibiting twinning, subparallel intergrowth and streaking of reflections, as is commonly reported for whiteite-group minerals (Moore and Ito, 1978; Marzoni Fecia Di Cossato *et al*., 1989; Grice *et al*., 1989). A reasonably clean crystal was obtained by slicing off subparallel minor laths with a scalpel. An intensity-data collection was carried out using a Bruker X8 Apex II CCD diffractometer equipped with monochromated Mo-*K*a radiation. The data collection conditions are given in Table 2. Data were processed using the *APEX II* program suite (Bruker, 2006).

The crystal-structure analysis was carried out using the *WinGX* suite of programs (Farrugia, 1999) for twinning (*ROTAX*) and cell

TABLE 1. EMP analyses (wt.%) of jahnsite–whiteite from Hagendorf Süd.

Association	—— Compact nordgauite ——			Fibrous nordgauite	Zwieselite-triplite	
Type	Whiteite	Whiteite	Jahnsite	Whiteite	Whiteite	Jahnsite
Number of analyses	Core (5)	Rim (5)	9	5	9	4
Figure references	1*a*, 2	1*a*, 2	1*b*	3	4	4
Na_2O	0.13	0.30	0.38	0.37	0.36	0.25
CaO	4.22	5.43	5.35	4.11	4.37	4.65
MnO	17.56	14.71	20.06	17.53	17.27	16.08
FeO	8.58	14.20	14.30	5.81	6.76	16.46
MgO	0.72	1.08	0.59	1.01	1.08	0.50
ZnO	0.48	1.11	0.66	3.51	3.47	1.99
P_2O_5	34.64	33.87	33.25	34.11	33.85	32.41
Al_2O_3	13.48	7.88	3.65	12.37	11.55	4.39
F	0.68	<d.l.	<d.l.	0.54	0.30	<d.l.
Total	80.49	78.58	78.24	79.36	79.01	76.73

Detection limit: 0.05 wt.%
Calculated formulae, normalized to 4P:
Whiteite (cores) in compact-form nordgauite: $Ca_{0.62}Na_{0.03}Mn_{2.03}Zn_{0.05}Fe_{0.98}Mg_{0.15}Al_{2.14}(PO_4)_4(OH_{1.71}\ F_{0.29}).8H_2O$
Whiteite (rims) in compact-form nordgauite: $Ca_{0.81}Na_{0.12}Mn_{1.74}Zn_{0.11}Fe_{1.66}Mg_{0.23}Al_{1.30}(PO_4)_4(OH)_2.8H_2O$
Jahnsite in compact form nordgauite: $Ca_{0.81}Na_{0.11}Mn_{2.40}Zn_{0.07}Fe_{1.73}Mg_{0.12}Al_{0.60}(PO_4)_4(OH)_2.8H_2O$
Whiteite in fibrous form nordgauite: $Ca_{0\cdot61}Na_{0.10}Mn_{2.06}Zn_{0.35}Fe_{0.67}Mg_{0.21}Al_2(PO_4)_4(OH_{1.76}F_{0.24}).8H_2O$
Whiteite in contact with zwieselite-triplite: $Ca_{0.65}Na_{0.10}Mn_{2.04}Zn_{0.35}Fe_{0.78}Mg_{0.22}Al_{1.90}PO_4)_4(OH_{1.87}\ F_{0.13}).8H_2O$
Jahnsite in contact with zwieselite-triplite: $Ca_{0.73}\ Na_{0.07}Mn_{1.98}Zn_{0.21}Fe_{2.01}Mg_{0.11}Al_{0.75}(PO_4)_4(OH)_2.8H_2O$

TABLE 2. Data-collection and refinement details for whiteite from Hagendorf Süd.

Ideal formula	$CaMn_3Al_2(PO_4)_4(OH,F)_2.8H_2O$
Crystal data	
Monoclinic cell parameters	
a, *b*, *c* (Å)	14.941(2), 6.9495(8), 10.054(1)
β (º)	111.00(1)
Z	2
Space group	*P*2/*a*
Calculated density	2.78 g cm^{-3}
Data collection	
Temperature (K)	293
λ (Mo-*K*α, Å)	0.7093
Crystal size (mm)	0.03 × 0.06 × 0.10
Collection mode	phi scan 360º, Δφ = 0.5º
Count time per frame	150 s
$2\theta_{max}$ (º)	60.98
No. of unique reflections	2713
No. of reflections, $I > 2.5\sigma(I)$	1015
Absorption correction (Multiscan)	μ = 2.73 mm^{-1}, T_{min}/T_{max} = 0.68
R_{merge} (observed)	0.08
Refinement	
No. of parameters refined	175
wR_{obs}, $I > 2.5\sigma(I)$	0.064
wR_{obs}, all data	0.088
GoF	1.22
Twinning	180º rotation about *a*
Twin volume fractions	0.701(6),0.299(6)
$\Delta\sigma_{min}$, $\Delta\sigma_{max}$ (e/Å^3)	−1.48, +1.94

transformation (*TRANSFORM*) and *JANA2000* (Petricek *et al*., 2000) for the refinements. The published coordinates for jahnsite-(NaFeMg) in space group *P*2/*a* (Kampf *et al*., 2008) were used as starting values for the refinement, with scattering curves for Ca, Mn, Mn and Al for the *X*, *M*(1), *M*(2) and *M*(3) sites, respectively. Application of *ROTAX* showed that twinning was probably due to 180º rotation about [100], the twin plane being (001). This twinning was implemented in *JANA2000*, and resulted in a reduction of wR_{obs} from 0.094 to 0.080. In the later stages of the refinement, the site occupancy factors at the *X* and *M* sites were refined. This showed greater scattering than Ca at the *X* site and Al at the *M*(3) sites, and less scattering than Mn at the *M*(2) sites. Fe was added to the *M*(3) sites and the proportions of Al and Fe refined. At the *M*(2) sites, the scattering curve for Fe was used to approximate the average of Mn, Fe and Zn, and the proportions of Fe and Mg were then refined. The final refinement using anisotropic displacement parameters converged to wR_{obs} = 0.064 (0.074 without twinning) for 1015 observed reflections with $I > 2.5\sigma(I)$. Because of the poor quality of the crystal, it was not possible to locate H atoms in difference Fourier maps. Other refinement details are given in Table 2. Refined parameters are reported in Table 3.

Results and discussion

SEM/EMP results

Back-scattered electron (BSE) images showing whiteite and/or jahnsite crystals in different mineral associations are presented in Figs 1–4. The EMP analytical results for each of these occurrences are listed in Table 1. Below Table 1 are reported the compositions from averaged analyses for each species, normalized to 4P.

Figure 1(*a*,*b*) shows the incorporation of whiteite (W) and jahnsite (J) within compact-

TABLE 3. Refined coordinates and equivalent isotropic displacement parameters.

Atom	Occupancy	*x*	*y*	*z*	U_{iso} (Å^2)
X	1.18(1)Ca	¼	0.9770(3)	0	0.032(1)
*M*1	1.0 Mn	¼	0.4798(3)	0	0.0150(8)
*M*2a	0.86(1)Fe*+ 0.14(1)Mg	½	0	½	0.0203(9)
*M*2b	0.85(2)Fe*+0.15(2)Mg	¼	0.4966(3)	½	0.0188(9)
*M*3a	0.80(2)Al+0.20(2)Fe	0	0	0	0.032(2)
*M*3b	0.96(1)Al+0.04(1)Fe	0	½	0	0.007(1)
*P*1	P	0.1786(2)	0.2574(3)	0.1859(3)	0.0167(8)
*P*2	P	0.0793(2)	0.7489(3)	0.8035(2)	0.0148(8)
O1	O	0.2707(5)	0.2319(10)	0.1503(7)	0.028(3)
O2	O	0.2007(5)	0.2870(9)	0.3415(7)	0.030(3)
O3	O	0.1178(5)	0.0771(9)	0.1342(8)	0.038(3)
O4	O	0.1315(5)	0.4353(9)	0.0956(7)	0.028(3)
O5	O	0.1879(4)	0.7087(10)	0.8547(7)	0.031(3)
O6	O	0.0420(5)	0.7766(8)	0.6450(6)	0.021(2)
O7	O	0.0681(5)	0.9307(9)	0.8809(7)	0.028(3)
O8	O	0.0282(5)	0.5867(8)	0.8407(7)	0.025(3)
O9	OH**	0.0222(4)	0.7506(8)	0.0792(6)	0.015(2)
O10	OW	0.2255(6)	0.7314(10)	0.3413(8)	0.040(3)
O11	OW	0.4532(6)	0.2157(9)	0.3393(7)	0.036(3)
O12	OW	0.6364(6)	0.9984(9)	0.4769(9)	0.036(3)
O13	OW	0.3955(6)	0.5121(8)	0.5074(9)	0.034(3)

* Fe scattering curve used to approximate Mn+Fe+Zn in *M*(2) sites
** OH and OW (water) oxygens assigned according to Kampf *et al*. (2008)

form nordgauite. A higher-magnification view in Fig. 2 of Fig. 1*a* shows details of the compositional zoning in the whiteite crystals. The interface between different compositional zones is sharp and follows the crystal boundaries, suggestive of a mineral-replacement reaction (Putnis, 2002). The mineral is very sensitive to electron-beam damage, as indicated by the white circle resulting from not defocusing the beam for analysis. Average analyses for the cores and rims are given in Table 1. The cores have darker BSE contrast, and have compositions close to that for end-member whiteite, whereas the lighter rims have greater Fe/Al ratios, corresponding to whiteite contents in the range 55 to 70%. In contrast, the crystals shown in Fig. 1*b*, from a different part of the same compact-form nordgauite nodule, are all richer in jahnsite, with jahnsite contents in the range 65−100%.

Inspection of the sectioned compact-form nordgauite nodule in a binocular microscope showed that the jahnsite−whiteite laths are colourless and transparent, similar in appearance to individual crystals from cavities. Underlying each cluster of crystals however, could be observed a larger dark-coloured inclusion. The small patches of bright phase on the left-hand side of Fig. 2 correspond to where the inclusion has reached the surface during polishing of the sample block. Analysis of this phase gives a composition $Fe_{1.6}Mn_{1.4}(PO_4)_2$. We were unable to obtain an XRD pattern of the minute amount of material, but the composition is consistent with graftonite, which occurs at Hagendorf and is a relatively common accessory primary phosphate in granitic pegmatites (Roda *et al*., 2004).

Whiteite laths were also found within fibrous-form nordgauite. A BSE image of part of a nordgauite spheroid is presented in Fig. 3. The whiteite laths do not display zoning as found for the laths within compact-form nordgauite. The EMPA results give a narrow range for Al_2O_3 (12.0 to 12.7 wt.%) corresponding to compositions clustered around the end-member formula. The fibrous-form nordgauite contains stringers of heavily corroded zwieselite-triplite primary phosphate. The EMP analysis of this phase gives a triplite-rich composition $Mn_{1.1}Fe_{0.8}Ca_{0.02}(PO_4)(F_{0.87}OH_{0.13})$. Other phases found in close association with fibrous-form nordgauite include

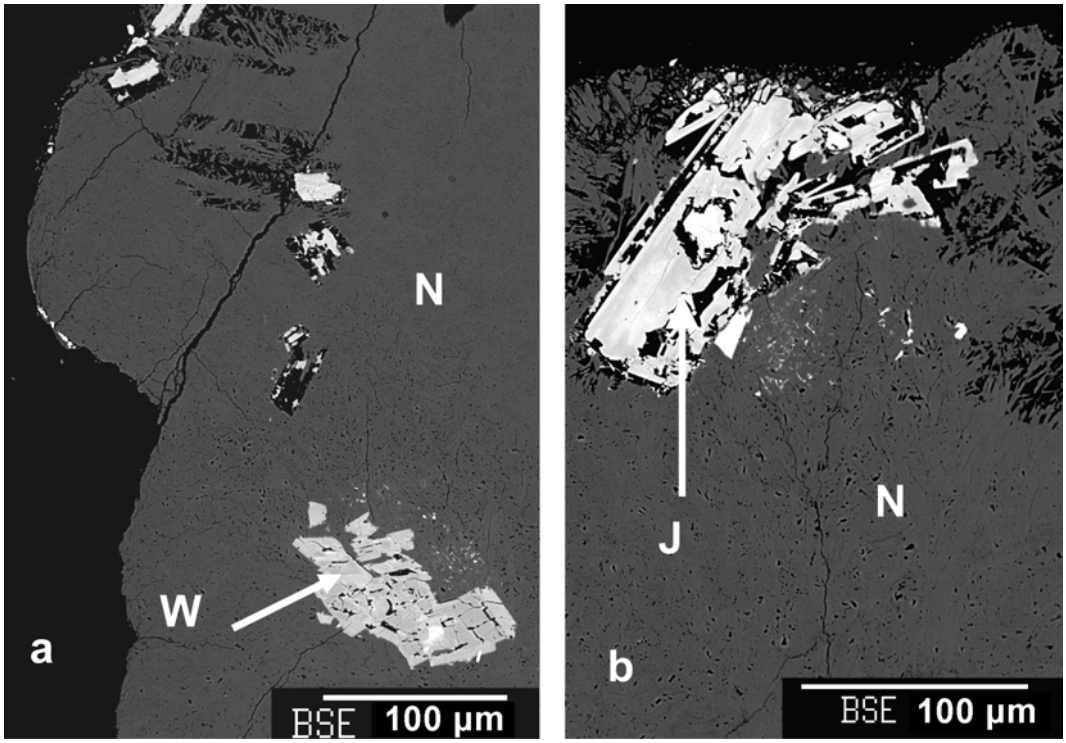

FIG. 1. BSE images of (*a*) whiteite (W) laths in compact-form nordgauite (N) and (*b*) jahnsite (J) laths in compact-form nordgauite.

Fe-bearing sphalerite, with a composition obtained from EMP analyses of $Zn_{0.9}Fe_{0.1}S$ and parascholzite, $CaZn_2(PO_4)_2.2H_2O$. The identity of the parascholzite was confirmed by single-crystal oscillation and precession studies.

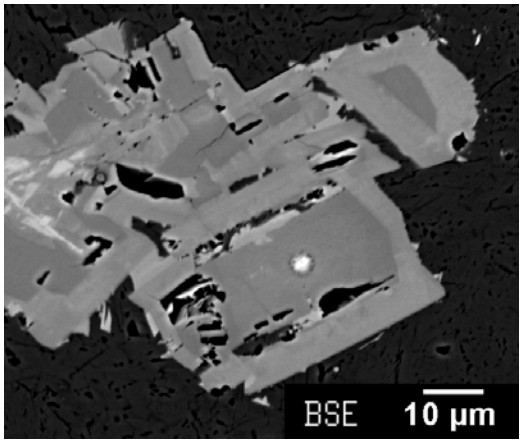

FIG. 2. Higher-magnification BSE view of the whiteite laths in Fig. 1*a* showing compositional zoning.

The spheroids of fibrous-form nordgauite commonly have a surface layer of very small, thin platelets of a mineral related to kingsmountite, $Ca_4(Fe,Mn)Al_4(PO_4)_6(OH)_4.12H_2O$ (Dunn *et al.*, 1979), as shown in Fig. 3. Analysis by EMP gave the composition:

$$[Ca_{3.64}Na_{0.02}Mn_{0.34}][Mn_{0.47}Fe_{0.21}Mg_{0.25}Zn_{0.07}][Al_{3.92}Fe_{0.08}](PO_4)_6(OH_{2.88}F_{1.12}).12H_2O.$$

The structural identity with kingsmountite and montgomeryite (Moore and Araki, 1974*a*) was confirmed by a powder XRD pattern. Mücke (1981) reported a Mn-bearing kingsmountite-related phase from the Hagendorf pegmatite as a coating on scholzite but noted that it contained no Al. Dunn *et al.* (1983) subsequently reported a similar encrustation on schozite crystals at Hagendorf and suggested, based on the large Fe content, that it was probably a new member of the kingsmountite/montgomeryite group with end-member formula $Ca_4MnFe_4(PO_4)_6(OH)_4.12H_2O$.

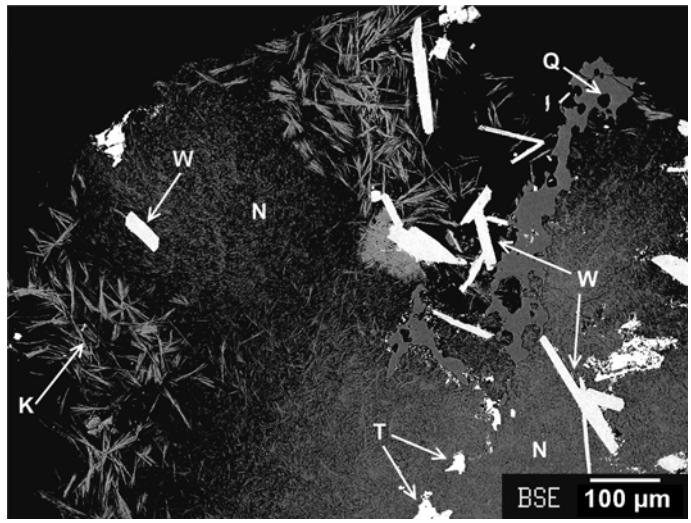

FIG. 3. BSE image of whiteite laths (W) in fibrous-form nordgauite (N). Associated triplite (T), quartz (Q) and a kingsmountite-related mineral (K) are labelled.

This member has subsequently been described from Mangualde, Portugal, and named zodacite (Dunn *et al.*, 1988). The mineral coating the surface of fibrous-form nordgauite differs from zodacite in being F-bearing and having Al as the dominant trivalent cation.

In addition to their association with nordgauite, zoned jahnsite–whiteite solid solution minerals were also found in close association with corroded groundmass zwieselite-triplite and apatite. An example is shown in Fig. 4. The jahnsite-rich compositions form at the edge of a large grain of uraninite (not shown in Fig. 4). Individual whiteite laths grow outwards on the LH side of Fig. 4, and are almost certainly the same as the crystal used for the structure analysis. Average analyses for the whiteite-rich and jahnsite-rich regions are given in Table 1. The whiteite is close to the end-member composition whereas the jahnsite is a solid solution of 63% jahnsite and 37% whiteite. Individual EMP analyses of different regions of both minerals show only small compositional variations. An EMP analysis of the zwieselite-triplite matrix gives the composition $(Mn_{0.96}Fe_{0.96}Ca_{0.03}Mg_{0.01})_{\Sigma 1.96}(PO_4)F_{0.78}OH_{0.22}$, halfway between zwieselite (M = Fe) and triplite (M = Mn) end-member compositions. The apatite is Mn-bearing with an EMP-derived composition of $(Ca_{4.78}Mn_{0.16}Fe_{0.02}Na_{0.01})_{\Sigma 4.97}(PO_4)_3F$.

The compositional variations within whiteite and jahnsite laths encased in compact-form nordgauite are illustrated in Fig. 5. The plot of the number of Al atoms per formula unit (p.f.u.)

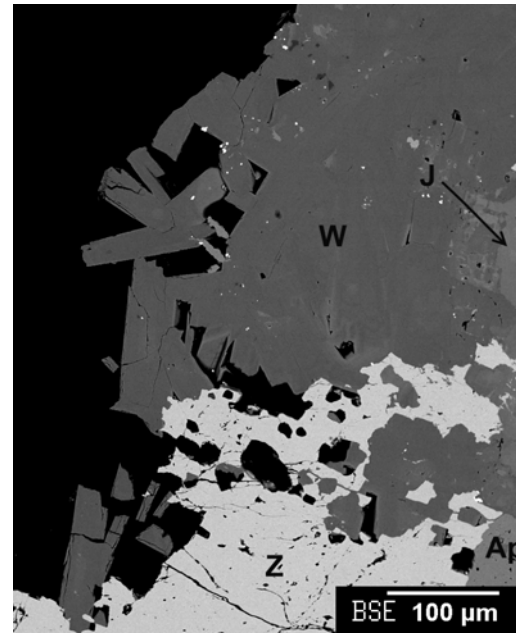

FIG. 4. BSE image of whiteite and jahnsite in contact with zwieselite-triplite (Z) and apatite (Ap).

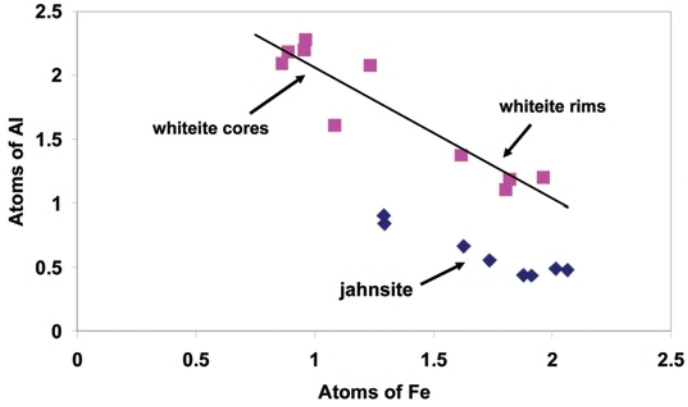

FIG. 5. Total number of Fe atoms p.f.u. *vs.* the number of Al atoms p.f.u. for whiteite and jahnsite laths in compact-form nordgauite.

vs. the total number of Fe atoms p.f.u. is based on individual EMP point analyses. The analyses for the whiteite-rich laths lie on a line of slope 1.0 (R^2 = 0.93), expected for substitution of Al-for-Fe in the *M*(3) site. The analyses for the jahnsite-rich laths are all displaced downwards, by an average 0.5 atoms p.f.u. A significant contributor to the smaller Fe/Al contents is the greater substitution of Mn for Fe in the jahnsite-rich laths, shown by the analyses in Table 1.

Apart from the obvious Fe^{3+}:Al^{3+} variations, the jahnsite-rich and whiteite-rich minerals display important differences. In particular, the whiteite laths were all found to be F-bearing whereas F is absent from the jahnsite laths, and the whiteite laths have compositions close to stoichiometric $(X,M)_6(PO_4)_4(OH,F)_2.8H_2O$ whereas the jahnsite occurrences are non-stoichiometric with $X+M \approx 5.85$. Such deficiencies in $X+M$ content appear to be common in EMP analyses of jahnsite–whiteite group minerals, *e.g.* $(X,M)_{5.77}P_4$ in whiteite-(CaMnMg) (Grice *et al.*, 1989), $(X,M)_{5.66}P_4$ in jahnsite-(CaMnMn) (Grice *et al.*, 1990) and $(X,M)_{5.54}P_4$ in jahnsite-(NaFeMg) (Kampf *et al.*, 2008). They could be due to electron beam damage, although in the present study both whiteite and jahnsite were analysed under identical conditions. Another possible explanation is the partial oxidation of divalent Fe in the Hagendorf jahnsites.

Whiteite crystal structure

The jahnsite-whiteite structure-type for the case of jahnsite has been described in detail by Moore and Araki (1974*b*) and more recently by Kampf *et al.* (2008) and so will only be described briefly here. It is one of the so-called 7 Å chain structures, containing [010] chains of *trans*-corner-connected $M(3)O_6$ octahedra, decorated with corner-connected PO_4 tetrahedra. Cross-linking of these chains along [100] to form (001) slabs occurs by chains of *trans*-connected alternating $M(3)O_6$ and $M(1)O_6$ octahedra. The $M(1)O_6$ octahedra share two edges with PO_4 from adjacent [100] chains. The *X* atoms occupy 8-coordinated (square antiprism) cavities within these slabs, giving a slab composition $XM(1)M(3)_2(OH)_2(PO_4)_4$. These slabs are bridged along [001] by corner sharing of the PO_4 tetrahedra to $M(2)(O,H_2O)_6$ octahedra.

Refinement of metal site occupancies for the whiteite crystal gave an *X*-site occupancy of 1.18(1) Ca, equivalent to 23.6(2) electrons and requiring a contribution from a heavier scatterer than Ca. Manganese is the largest of the available heavier atoms and commonly substitutes for Ca. Location of Mn+Ca at the *X* site, however, requires 0.26 Ca+0.74 Mn to match the refined number of electrons at the site. Such a small Ca content is quite inconsistent with the EMP analyses reported in Table 1. If Zn is substituted at the *X* site, the refined number of electrons is matched with 0.73Ca+0.37Zn. The resulting Ca and Zn contents are both in good agreement with EMP analyses for whiteite in contact with zwieselite-triplite in Table 1, and will only be changed slightly if a small amount of Na is included at the *X* site. This result is surprising as Zn is much smaller than Ca and Ca-Zn phosphates

such as parascholzite, found in close association with whiteite, show no mixing of Ca and Zn in the same site (Taxer and Bartl, 1997). The assignment agrees, however, with that reported from a crystal-structure refinement of whiteite from Hagendorf by Chernyatieva *et al*. (2010). The refined amounts of Mg at *M*(2) sites (0.29(3)Mg p.f.u.), and Fe at *M*(3) sites (0.24(3)Fe p.f.u.) are also in reasonable agreement with EMP analyses for whiteite in contact with zwieselite-triplite in Table 1.

Polyhedral bond lengths from the whiteite single-crystal refinement are reported in Table 4. The crystal-chemical data are generally quite consistent, although the results for the Al-rich *M*(3) sites are contradictory and may reflect the poor quality of the crystal and associated twinning. The longer average bond length for *M*(3b) (1.90 Å) and its lower isotropic displacement parameter (0.007 $Å^2$) relative to *M*(3a) (1.88 Å and 0.032 $Å^2$) suggest that any Fe substitution will be greater at the *M*(3b) site. The refined site occupancies in Table 3, however, show the reverse. The average P−O distances of 1.53 and 1.51 Å are slightly shorter than the range of 1.53 to 1.54 Å reported for jahnsites (Moore and Araki, 1974b; Kampf *et al*., 2008). The average *M*(1)−O distance of 2.23 Å is greater than those for *M*(2)−O, 2.11 Å and 2.15 Å, consistent with Mn^{2+} being ordered in *M*(1) and being mixed with smaller cations such as Fe^{2+} and Mg^{2+} in the *M*(2) sites. The *X* site has the same coordination as reported for jahnsite-(NaFeMg), with six distances of <2.57 Å and two longer *X*−O distances at 2.85 Å.

Conclusions

Minerals of the jahnsite−whiteite group, associated with nordgauite in the Hagendorf Süd granitic pegmatite, are commonly zoned and their compositions cover the full compositional range between the two end-members. Whiteite-rich compositions are F-bearing and stoichiometric, while compositions with increasing Fe content have little or no F and are metal-deficient, possibly due to divalent Fe being partially oxidized to the trivalent state. The gradation of low-Fe to high-Fe compositions occurs from centres to edges of the mineral occurrences, suggesting that whiteite formed first and was subsequently transformed to more Fe-rich compositions, with associated removal of F.

Compositional features common to the secondary phosphate minerals identified in the present study are large Mn contents and, except for jahnsite, the incorporation of F. These elements are present in the associated primary minerals zwieselite-triplite and Mn-bearing fluorapatite. Dill *et al.* (2008) suggested that the

TABLE 4. Polyhedral bond lengths (Å) for whiteite from Hagendorf Süd.

Ca−O1 (×2)	2.277(7)	*M*3a−O3 (×2)	1.872(6)
Ca−O3 (×2)	2.849(9)	*M*3a−O7 (×2)	1.890(9)
Ca−O5 (×2)	2.345(7)	*M*3a−O9 (×2)	1.886(5)
Ca−O7 (×2)	2.568(7)		
*M*1−O1 (×2)	2.239(7)	*M*3b−O4 (×2)	1.906(6)
*M*1−O4 (×2)	2.317(8)	*M*3b−O8 (×2)	1.895(8)
*M*1−O5 (×2)	2.134(7)	*M*3b−O9 (×2)	1.894(5)
*M*2a−O6 (×2)	2.068(6)	*P*1−O1	1.551(8)
*M*2a−O11 (×2)	2.130(7)	*P*1−O2	1.493(8)
*M*2a−O12 (×2)	2.133(10)	*P*1−O3	1.525(7)
		*P*1−O4	1.546(7)
*M*2b−O2 (×2)	2.088(7)		
*M*2b−O10 (×2)	2.219(8)	*P*2−O5	1.542(7)
*M*2b−O13 (×2)	2.152(9)	*P*2−O6	1.500(6)
		*P*2−O7	1.525(7)
		*P*2−O8	1.482(7)

jahnsite–whiteite minerals originated from the decomposition of apatite in the Silvergrübe Aplite at Hagendorf. In associations of jahnsite-whiteite/zwieselite-triplite/apatite as shown in Fig. 4, the zwieselite-triplite has a corroded appearance and may be the precursor to the whiteite. Strongly corroded triplite is also a residual phase in fibrous-form nordgauite containing whiteite crystals, as shown in Fig. 3. The ubiquitous presence of F in the secondary phosphate minerals whiteite, nordgauite and kingsmountite-type in the samples studied here is not thought to have a structural explanation, but is simply due to its availability during the crystallization of these minerals. The phosphates were also found to have significant incorporation of Zn, with ZnO contents ranging up to 4.2 wt.% in whiteite. Crystals of the Zn-rich phosphate, parascholzite, were found in close association with the nordgauite/jahnsite–whiteite assemblages. In other parts of the Hagendorf Süd pegmatite, sphalerite-derived Zn-phosphate minerals are common and include scholzite, phosphophyllite and hopeite (Mücke, 1981).

Moore and Ito (1978) proposed a scheme to distinguish different species of jahnsite–whiteite, in which, after assignment of Fe/Al to *M*(3), the sites *M*(2), *M*(1) and *X* are successively filled with cations of increasing radius. The jahnsite or whiteite species is then designated by the dominant cation in these sites as –(*XM*(1)*M*(2)). Our refinement of whiteite contradicts this scheme inasmuch as the relatively small Zn^{2+} cation appears to be substituting with Ca^{2+} in the *X* site. Taking the structure refinement results into account, the average EMP analyses for whiteite in contact with zwieselite-triplite can be presented as the structural formula:

$$[Ca_{0.65}Na_{0.10}Zn_{0.25}][Mn][Mn_{1.00}Fe_{0.68}Mg_{0.22}Zn_{0.10}][Al_{1.9}Fe_{0.1}](PO_4)_4(OH_{1.87}F_{0.13}).8H_2O$$

According to the Moore and Ito (1978) scheme, this corresponds to whiteite-(CaMnMn). A CaMnMn-dominant whiteite end-member has recently been reported from the Hagendorf pegmatite by Chernyatieva *et al*. (2010). The whiteite found in fibrous-form nordgauite is also this species. The jahnsite crystals, found both within compact-form nordgauite and in contact with zwieselite-triplite conform to jahnsite-(CaMnMn), which has been previously reported from Mangualde, Portugal, by Grice *et al*. (1990). The whiteite found within compact-form nordgauite is a new species, whiteite-(CaMnFe), that has not previously been approved by the IMA CNMNC. Unfortunately, to date we have been able to locate only one very small occurrence of zoned crystals shown in Fig. 2. Further searching is warranted to obtain unzoned crystals suitable for characterization, in order to prepare a new-mineral proposal. The kingsmountite-related mineral found as an encrustation on fibrous-form nordgauite also appears to be a new CaMnAl species. Further data are being assembled on this phase with a view to submitting a new-mineral proposal to the IMA CNMNC.

Acknowledgements

The authors thank Erich Keck for supplying specimens from the Hagendorf Süd pegmatite. Thanks to Monash University Chemistry Department for providing access to their Bruker Apex II diffractometer, and to Ludmilla Malishev and Cameron Davidson for EMP sample preparation.

References

Birch, W.D., Grey, I.E., Mills, S.J., Pring, A., Wilson, N.C. and Keck, E. (2010) Nordgauite, $MnAl_2(PO_4)_2(F,OH)_2.5.5H_2O$, a new mineral from the Hagendorf Süd pegmatite, Bavaria, Germany. *Mineralogical Magazine*, *submitted*.

Bruker (2006) *Apex-II, Area detector software package* v2.1. Bruker Analytical X-ray Systems Inc., Madison, Wisconsin, USA.

Chernyatieva, A.P., Krivovichev, S.V., Yakovenchuk, V.N. and Pakhomovsky, Y.A. (2010) Crystal chemistry of a new CaMnMn-dominant member of the whiteite group. *Abstracts, IMA2010, 20th General Meeting of the International Mineralogical Association*, August, 2010, Budapest, Hungary. *Acta Mineralogica-Petrographica* Abstract Series, Volume **6**, p. 716, Department of Mineralogy, Geochemistry and Petrology, University of Szeged, Hungary.

Dill, H.G., Weber, B., Gerdes, A. and Melcher, F. (2008) The Fe-Mn phosphate aplite 'Silbergrube' near Waidhaus, Germany: epithermal phosphate mineralization in the Hagendorf-Pleystein province. *Mineralogical Magazine*, **72**, 1119–1144.

Dunn, P.J., Peacor, D.R., White, J.S. and Ramik, R.A. (1979) Kingsmountite, a new mineral isostructural with montgomeryite. *The Canadian Mineralogist*, **17**, 579–582.

Dunn, P.J., Roberts, W.L., Campbell, T.J. and Leavens, P.B. (1983) Red montgomeryite and associated minerals from the Tip Top Pegmatite with notes on kingsmountite and calcioferrite. *The Mineralogical*

Record, May-June, 195–197.

Dunn, P.J., Grice, J.D. and Metropolis, W.C. (1988) Zodacite, the Mn analogue of montgomerytite, from Mangualde, Portugal. *American Mineralogist*, **73**, 1179–1181.

Farrugia, L.J. (1999) *WinGX* suite for small-molecule single-crystal crystallography. *Journal of Applied Crystallography*, **32**, 837–838.

Grice, J.D., Dunn, P.J. and Ramik, R.A. (1989) Whiteite-(CaMnMg), a new mineral species from the Tip Top pegmatite, Custer, South Dakota. *The Canadian Mineralogist*, **27**, 699–702.

Grice, J.D., Dunn, P.J. and Ramik, R.A. (1990) Jahnsite-(CaMnMn), a new member of the whiteite group from Mangualde, Beira, Portugal. *American Mineralogist*, **75**, 401–404.

Kampf, A.R., Steele, I.M. and Loomis, T.A. (2008) Jahnsite-(NaFeMg), a new mineral from the Tip Top mine, Custer County, South Dakota: Description and crystal structure. *American Mineralogist*, **93**, 940–945.

Kastning, J. and Schlüter, J. (1994) Die mineralien von Hagendorf und ihre bestimmung. Schriften des mineralogischen museums der Universität Hamburg, Band 2, C. Weise Verlag, Munich, Germany, 95 pp.

Marzoni Fecia Di Cossato, Y., Orlandi, P. and Vezzalini, G. (1989) Rittmannite, a new mineral species of the whiteite group from the Mangualde granitic pegmatite, Portugal. *The Canadian Mineralogist*, **27**, 447–449.

Moore, P.B and Araki, T. (1974*a*) Montgomeryite, $Ca_4Mg(H_2O)_{12}[Al4(OH)_4(PO_4)_6]$: Its crystal structure and relationship to vauxite, $Fe_2^{2+}(H_2O)_4[Al_4(OH)_4(PO_4)_4].4H_2O$. *American Mineralogist*, **59**, 843–850.

Moore, P.B. and Araki, T. (1974*b*) Jahnsite, $CaMn^{2+}Mg_2(H_2O)_8Fe_2^{3+}(OH)_2[PO_4]_4$: A novel stereoisomerism of ligands about octahedral corner-chains. *American Mineralogist*, **59**, 964–973.

Moore, P.B. and Ito, J. (1978) I. Whiteite, a new species, and a proposed nomenclature for the jahnsite–whiteite complex series. II. New data on xanthoxenite. III. Salmonsite discredited. *Mineralogical Magazine*, **42**, 309–323.

Mücke, A. (1981) The paragenesis of the phosphate minerals of the Hagendorf pegmatite – a general view. *Chemie de Erde/Geochemistry*, **40**, 217–234.

Petricek, V., Dusek, M. and Palatinus, L. (2000) *Jana2000*. Structure Determination Software Programs, Institute of Physics, Praha, Czech Republic.

Putnis, A. (2002) Mineral replacement reactions: From macroscopic observations to microscopic mechanisms. *Mineralogical Magazine*, **66**, 689–708.

Roda, E., Pesquera, A., Fontan, F. and Keller, P. (2004) Phosphate mineral associations in the Canada pegmatite (Salamanca, Spain): Paragenetic relationships, chemical compositions, and implications for pegmatite evolution. *American Mineralogist*, **89**, 110–125.

Taxer, K. and Bartl, H. (1997) Die "geordnete gemittelte" kristallstruktur von parascholzit. Zur dimorphie von $CaZn_2(PO_4)_2.2H_2O$, parascholzit-scholzit. *Zeitschrift für Kristallographie*, **212**, 197–202.